AGU PUBLICATIONS

JGR

Journal of Geophysical Research: Atmospheres

RESEARCH ARTICLE

10.1002/2013JD020818

Key Points:

- Mass balance and stable oxygen isotope ratios from shallow firn cores
- Decreasing trend in surface mass balance, no trend in stable isotopes
- Negative correlation between SAM and SMB

Correspondence to:
E. Schlosser,
Elisabeth.Schlosser@uibk.ac.at

Citation:
Schlosser, E., H. Anschütz, D. Divine, T. Martma, A. Sinisalo, S. Altnau, and E. Isaksson (2014), Recent climate tendencies on an East Antarctic ice shelf inferred from a shallow firn core network, *J. Geophys. Res. Atmos.*, *119*, 6549–6562, doi:10.1002/2013JD020818.

Received 3 SEP 2013
Accepted 20 MAY 2014
Accepted article online 24 MAY 2014
Published online 11 JUN 2014

Recent climate tendencies on an East Antarctic ice shelf inferred from a shallow firn core network

E. Schlosser[1], H. Anschütz[2], D. Divine[3], T. Martma[4], A. Sinisalo[5], S. Altnau[1], and E. Isaksson[3]

[1]Institute of Meteorology and Geophysics, University of Innsbruck, Innsbruck, Austria, [2]NGI Oslo, Oslo, Norway, [3]Norwegian Polar Institute, Fram Centre, Tromsø, Norway, [4]Institute of Geology, Tallinn University of Technology, Tallinn, Estonia, [5]Department of Geosciences, University of Oslo, Oslo, Norway

Abstract Nearly three decades of stable isotope ratios and surface mass balance (SMB) data from eight shallow firn cores retrieved at Fimbul Ice Shelf, East Antarctica, in the Austral summers 2009–2011 have been investigated. An additional longer core drilled in 2000/2001 extends the series back to the early eighteenth century. Isotope ratios and SMB from the stacked record of all cores were also related to instrumental temperature data from Neumayer Station on Ekström Ice Shelf. Since the second half of the twentieth century, the SMB shows a statistically significant negative trend, whereas the $\delta^{18}O$ of the cores shows a significant positive trend. No trend is found in air temperature at the nearest suitable weather station, Neumayer (available since 1981). This does not correspond to the statistically significant positive trend in Southern Annular Mode (SAM) index, which is usually associated with a cooling of East Antarctica. SAM index and SMB are negatively correlated, which might be explained by a decrease in meridional exchange of energy and moisture leading to lower precipitation amounts. Future monitoring of climate change on the sensitive Antarctic ice shelves is necessary to assess its consequences for sea level change.

1. Introduction

The polar regions play an important role in the climate system. Positive feedbacks (e.g., ice-albedo feedback) lead to reactions to changes in the climate system that are more pronounced in the Arctic and Antarctic than at lower latitudes. Generally, the Arctic exhibits the most distinct temperature increase during recent decades [*Solomon et al.*, 2007]. However, regionally, the strongest temperature rise has been observed in the Antarctic Peninsula region. Most recent investigations [e.g., *Bromwich et al.*, 2013] show that also the central West Antarctic ice sheet belongs to the most rapidly warming regions on our planet. The large ice mass of Antarctica is in particular a critical factor concerning sea level rise in a warming climate. An increase in mass balance could mitigate sea level rise.

Since temperatures on mainland Antarctica are mostly considerably below the freezing point, even several degrees of warming would not lead to any snow melt. The surrounding ice shelves, however, are more sensitive to climate change since they already have a surface temperature regime that is close to the melting point in summer. But the mass balance depends on both ice dynamic effects [*Pritchard et al.*, 2009, 2012; *Jenkins et al.*, 2010] and direct atmospheric influences, namely, temperature and precipitation. Additionally, the oceanic circulation underneath the ice shelf plays a role that is so far only partly understood [*Hattermann et al.*, 2012]. Changes in surface mass balance (SMB) and also the total mass balance of the ice shelves influence ice dynamics and thus discharge of ice from the continent. A reduction of ice shelf thickness and extent limits its ability to buttress the flow of tributary glaciers, leading to accelerated ice discharge. This has been found not only in West Antarctica but also for several ice shelves in East Antarctica, among them the relatively large Amery and Shackleton Ice Shelves [*Pritchard et al.*, 2012]. *Rignot et al.* [2013] report that nearly half of the East Antarctic ice shelves are thinning due to increased basal melt. In West Antarctica, ice mass loss is clearly increasing due to accelerated glacier flow after disintegration of ice shelves both in the Antarctic Peninsula [e.g., *Rott et al.*, 2002, 2007] and along the Amundsen Sea coast [*Rignot*, 2008; *Park et al.*, 2013]. There is increasing evidence for the importance of the oceanic influence on the mass balance, namely, on thickness and flow of ice shelves [*Jacobs et al.*, 2011; *Pritchard et al.*, 2012; *Depoorter et al.*, 2013]. A recent study of *Bintanja et al.* [2013] points out that increased basal melting of Antarctic ice shelves also influences sea ice extent by changing the stratification of the ocean.

Therefore, a close monitoring of the conditions in the coastal zones of Antarctica is necessary to detect early signs of climate change and its consequences for the mass balance of Antarctica and global sea level.

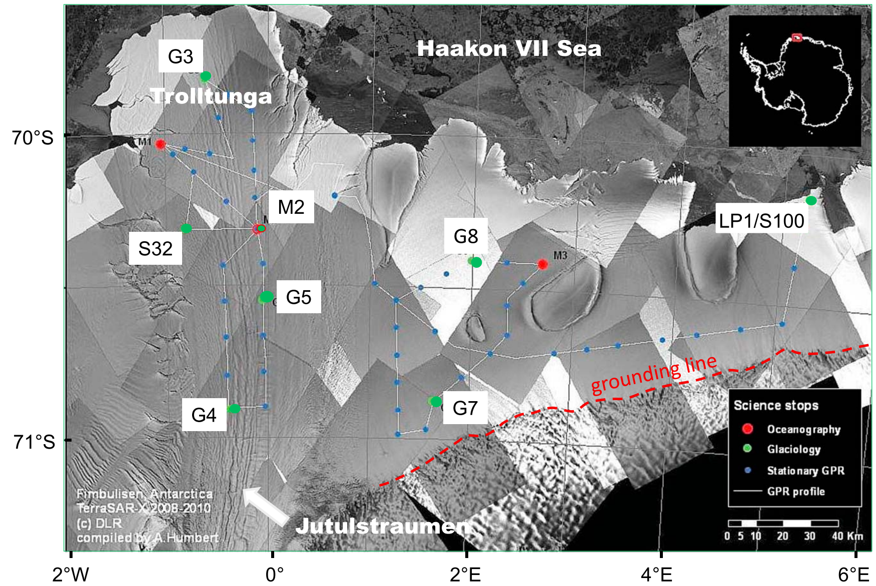

Figure 1. Map of investigation area (Fimbulisen, East Antarctica), showing the traverse route/GPR profiles (white line) and the location of firn cores (green circles). The grounding line is indicated as dashed red line. The underlying image is from a TerraSar image, courtesy of DLR, compiled by A. Humbert.

In addition, studies of the processes relevant for today's SMB using modern data can contribute to a better understanding of data from ice cores. In this study, data from eight firn cores taken on Fimbul Ice Shelf, East Antarctica, are used to investigate both possible changes/trends in SMB of the ice shelf and the relationship between SMB and air temperature/δ^{18}O. Large-scale atmospheric influences such as the Southern Annular Mode (SAM) as the dominant climate mode at high southern latitudes are examined. We focus here on the past three decades, the period for which the effect of possibly anthropogenically induced global changes became apparent. The data are also considered in a longer-term context using the core from the area that was recovered earlier.

2. Field Area

With an area of approximately 33,000 km^2, Fimbul Ice Shelf (also known as Fimbulisen) is one of the largest ice shelves bounding Dronning Maud Land (DML), East Antarctica, at the shore of the Haakon VII Sea (Figure 1). It stretches approximately 100 km north-south between 69.5°S and 71.5°S and 200 km east-west between 3°W and 4°E, respectively. The ice shelf includes a number of ice rises, varying in size between 15 km^2 and approximately 1200 km^2, the larger ones locally influencing the SMB by lee or upwind effects [*Sinisalo, et al*., 2013]. The central part of Fimbul Ice Shelf is nourished by Jutulstraumen, a fast-flowing ice stream that drains an area of 124,000 km^2 and represents the largest outlet glacier in Dronning Maud Land. The continuation of Jutulstraumen is a fast-moving tongue within the ice shelf, called Trolltunga, that is surrounded by ice moving more slowly to the east and west, causing highly crevassed areas on both sides due to high shear stress. The ice velocity at the grounding line amounts to about 1 km/yr. In the north, Trolltunga projects as ice peninsula into the Haakon VII Sea, which causes an accumulation regime slightly different from the rest of the ice shelf since the surrounding ocean water leads to higher air temperatures; also, higher wind speeds are expected at this peninsula. Generally, Fimbulisen, as most East Antarctic ice shelves, is under the climatic influence of the circumpolar trough, with cyclones passing frequently and bringing precipitation connected to frontal systems.

3. Previous Work

The first scientific investigations on Fimbul Ice Shelf took place during the British-Norwegian-Swedish Expedition in 1949–1952 [*Swithinbank*, 1957]. Between 1956 and 1960, glaciological research was conducted at Norway Station (later called SANAE), which was situated on the western edge of the ice shelf [*Lunde*, 1961].

Neethling [1970] investigated the SMB using accumulation stake measurements at arrays and along traverses as well as stratigraphic studies on snow pits and firn cores. They noticed a positive trend in SMB between 1913 and 1960. Different from later studies, accumulation maxima were found in fall and winter rather than in fall and spring, the latter related to equinoctial pressure minima associated to the semiannual oscillation (SAO) [*Van Loon*, 1967]. They also stress the—for an ice shelf rather unusual—katabatic wind influence, evident from the relatively high frequency of winds from the SE sector at Norway Station/SANAE, caused by the interaction and superimposition of katabatic winds and late-stage cyclonic winds.

Since 1976/1977, various Norwegian groups have worked on Fimbulisen and Jutulstraumen as part of NARE (Norwegian Antarctic Research Expedition) [e.g., *Isaksson and Melvold*, 2002; *Melvold et al.*, 1998; *Melvold*, 1999; *Rolstad et al.*, 2000]. During NARE 2000/2001, a 100 m deep ice core called S100 was drilled on the eastern part of Fimbul Ice Shelf (Figure 1) [*Kaczmarska et al.*, 2004]. This core covers the period of 1737–2000 A.D. ± 3 years and is the longest among the available high-resolution records from this part of coastal DML. *Kaczmarska et al.* [2004] found higher accumulation rates in the nineteenth century than in the eighteenth and twentieth century. *Kaczmarska et al.* [2006] then related the number of melt layers per year in S100 to stable oxygen isotope ratios and to air temperature from four meteorological stations (Halley, Neumayer, Syowa, and Novolazarevskaya). They found no straightforward relationship between those variables.

Divine et al. [2009] used eight cores (including S100) from coastal DML to investigate the role of the tropical El Niño-Southern Oscillation (ENSO) and the Southern Annular Mode (SAM) in the temporal variability of δ^{18}O in the area. They found that on typical ENSO timescales of 2–6 years, the strength of the teleconnection varies in time, being stronger for years with a generally negative phase of the SAM.

Rotschky et al. [2007] compiled a surface accumulation map for western Dronning Maud Land, which includes Fimbul Ice Shelf. They used a special interpolation scheme to derive this map using data from firn/ice cores and snow pits. However, at that time, data density on Fimbulisen was fairly low but has since then considerably increased through the most recent Norwegian expeditions.

4. Data and Methods

An extensive field program was carried out on Fimbul Ice Shelf in the frame of two expeditions in Austral summers 2009/2010 and 2010/2011 in order to investigate the recent mass balance of the ice shelf and reveal a possible local response to the ongoing global climatic changes. It was part of the oceanographic/glaciological project "Fimbul Ice Shelf—from top to bottom" (http://fimbul.npolar.no) that aimed at understanding the interaction between the Antarctic ice sheet and the ocean. The project is a cooperation between oceanographers and glaciologists and combines glaciological measurements of the SMB [*Schlosser et al.*, 2012; *Sinisalo et al.*, 2013] and basal topography of the ice shelf [*Langley et al.*, 2014] with oceanographic methods [*Hattermann et al.*, 2012] and modeling (T. Hattermann et al., Eddy-resolving simulations of the Fimbul ice shelf cavity circulation: Basal melting and exchange with open ocean, *Ocean Modelling*, under revision, 2013), to determine the mass balance at both the bottom and the surface of the ice shelf. This effort included drilling of eight shallow firn cores, stake measurements for determination of ice velocity and SMB, ground-penetrating radar measurements (GPR), and hot-water drilling for deployment of oceanographic instruments underneath the ice shelf. First results of the SMB study have been published after the analysis of the first four firn cores, G3, G4, G5, and M2 (Group 1), all situated on the western part of Fimbul Ice Shelf [*Schlosser et al.*, 2012]. (The analysis of the remaining cores, G7, G8, LP1, and S32 (Group 2), was carried out afterward.) In this study, we present a comprehensive study of both the SMB and δ^{18}O data from all available firn cores. One of these cores has been drilled at the same location as S100, thus extending the time series from 1737 [*Kaczmarska et al.*, 2004] to the present. We mainly focus on possible climatic trends in SMB as well as the relationship between SMB and stable oxygen isotopes/air temperature viewed in a broader climatic context. In particular, we are interested in their possible relation to the Southern Annular Mode (SAM) [*Marshall*, 2003].

Figure 1 shows the traverse route (GPR profiles) and the location of shallow firn cores and hot water drillings for oceanographic measurements on Fimbul Ice Shelf. Table 1 gives coordinates and metadata of the firn cores.

4.1. Stable Oxygen Isotope Ratios

Stable oxygen isotope ratios (δ^{18}O) of the firn cores G3, G4, G5, M2, and LP1 (melted samples) were analysed in the Laboratory of Mass Spectrometry at the Institute of Geology, Tallinn University of Technology, Estonia,

Table 1. Location and Metadata of Firn Cores G3, G4, G5, M2, G7, G8, S32, and LP1[a]

Firn Core	Lat. (°S)	Lon.	Elev. (m a.s.l.)	Length (m)	Time Period	Mean Annual SMB (mm w.e.)	Trend Magnitude 1995–2009 (mm w.e. yr^{-1})	Trend Magnitude (mm w.e. yr^{-1})
G3	69.823	0.612°W	57	10.0	1993–2009	295(29)	−7(7)	−10(6)
M2	70.316	0.109°W	73	17.5	1981–2009	315(22)	−13(6)	**−7(2)**
G5	70.545	0.041°W	82	14.5	1983–2009	298(21)	−8(6)	−1(3)
G4	70.902	0.402°W	60	16.7	1983–2009	330(21)	−6(5)	**−8(2)**
G7	70.87	1.65°E	55	16.1	No dating	208(3)	—	—
G8	70.41	2.01°E	58	10.7	1991–2009	282(26)	−9(6)	−7(5)
S32	70.31	0.80°W	53	10.0	1995–2009	339(36)	**−21(6)**	**−21(6)**
LP1	70.233	4.800°E	48	11.0	1992–2009	296(33)	−11(7)	−6(6)
S100	70.233	4.800°E	48	100	1737–1999	290(10)	—	0(0.1)

[a]LP1 was drilled at the same location as S100 [*Kaczmarska et al.*, 2004]. The covered time periods correspond to the dating using seasonal variations of stable isotope ratios combined with DEP measurements. Mean annual SMB for all firn cores and corresponding linear trends are given. Uncertainties of the calculated average SMB values and standard deviations of trend magnitudes are given in parenthesis. Trend magnitudes statistically significant at the 95% confidence level according to *F* test are highlighted in bold. Significance testing was done with respect to a null hypothesis of no trend in the data; serial correlation in the residuals of the linear model was taken into account via estimation of the effective sample size following *Mitchell et al.* [1966]. For G7, no trend was calculated since an exact determination of annual layers was not possible due to several missing annual layers. Thus, only the mean SMB between 1983 and 2009 is given, assuming that the largest peak in the DEP profile corresponds to the El Chichon volcanic eruption (confirmed by radar measurements).

using a Thermo Fisher Scientific Delta V Advantage mass spectrometer with Gasbench II. The reproducibility of replicate analysis for the $\delta^{18}O$ measurements is ±0.1 ‰. G7, G8, and S32 were also analysed in Tallinn using a Picarro L2120-i Isotopic Liquid Water Analyser with High-Precision Vaporizer A0211. S100 was analysed with a mass spectrometer (VG ISOGAS) at the University of Copenhagen [*Kaczmarska et al.*, 2004]. S100 is by far the longest/oldest core of this study area. No flow correction was applied to the data, however, since the terrain upstream of the drilling site is fairly flat, so that the older parts of the core originate from areas of only slightly higher altitude. The isotope ratios are given in the common delta notation relative to Vienna-Standard Mean Ocean Water (V-SMOW). The sampling interval was 5 cm, which ensures that a good subannual resolution is given. An annual accumulation in the order of magnitude 300 mm w.e. (typical for the area) [*Schlosser et al.*, 2012] corresponds to approximately 10–12 samples per year.

4.2. Dielectric Profiling

For all cores, dielectric profiling (DEP) measurements were conducted in the cold laboratory of the Norwegian Polar Institute, Tromsø, Norway. The measuring interval was 5 mm, the temperature was held constant at −20°C. The accuracy of the measurements is approximately ±1% [*Wilhelms et al.*, 1998]. Since the AC conductivity reflects seasonal variations of various ions in the firn, it can be used for dating of the cores by counting annual layers. However, apparent summer peaks can as well be due to sea salt maxima from single-storm events. Thus, the method has to be used with care. In cores, for which no stable isotope data are available or the seasonal variations of $\delta^{18}O$ cannot be resolved, DEP data are often used to identify peaks of volcanic origin as time markers, to be able to calculate the mean accumulation rate between the found volcanic eruptions. Yet these peaks can also be associated with other processes, such as maxima in the deposition of sea salt or other ions not related to volcanic eruptions. For an unambiguous definition of the volcanic time markers, additional information (e.g., volcanic ash (tephra) layers) is required. For the Fimbul cores, this information is not available. Details about the underlying physics of DEP as well as the measuring device can be found in *Glen and Paren* [1975], *Moore et al.* [1989], *Wilhelms* [2005], and *Wilhelms et al.* [1998].

4.3. Stake Measurements

Along the traverse route, stake measurements were carried out in four summer seasons. Details about those data can be found in *Sinisalo et al.* [2013]. Three years of stake measurements is obviously a too short time period to conclude anything about temporal variability of SMB. However, it turned out that 2009 and 2010 have been two extreme years in terms of accumulation in East Antarctica, 2009 being a relatively warm, high-accumulation year, whereas 2010 was cold and dry compared to the average [e.g., *Boening et al.*, 2012; *Gorodetskaya et al.*, 2013; *Lenaerts et al.*, 2013], so that the data give a general idea about both the range and the spatial variability of SMB (without taking single values too literally). For our study, it is important that negative SMB values occurred due to wind erosion, namely, in the vicinity of G7, which could not be dated since several annual layers were entirely missing.

4.4. Climatological Data

Since the stable isotope ratio not only depends on air temperature but is also influenced by a considerable number of other parameters, it would be desirable to have measured air temperatures from Fimbul Ice Shelf or as close as possible for comparison.

The abovementioned year-round base SANAE, which was situated on Fimbul Ice Shelf itself (70°18′S/2°22′W), provides data only until 1992. The German Neumayer Station on Ekströmisen (70°39′S/8°15′W), a small ice shelf approximately 200 km further west, was built in 1981 and has been in operation until today. Data from the British base Halley, which are available since the International Geophysical Year (1957/1958) and have been used in previous studies for comparison with ice cores, are not used in our study since the meteorological regime of Halley is too different from the conditions at Fimbul Ice Shelf. Halley is situated much further south (75°35′S/26°34′W) and strongly influenced by the year-round ice-covered Weddell Sea, which has consequences for both temperature and general atmospheric flow. The next station close to Fimbul Ice Shelf to the East is the Russian base Novolazarevskaya. However, Novolazarevskaya is situated in an oasis rather than on an ice shelf and has a fairly particular local climate, which is altered by snow-free rocks and thus very different from SANAE and Neumayer, even though they are all under the same synoptic influences. Therefore, different from earlier studies by *Kazcmarska et al.* [2004] and *Isaksson et al.* [1999], for comparison with $\delta^{18}O$ profiles of the shallow firn cores, we use annual mean air temperature only from Neumayer Station (1981–2010) calculated from the 3-hourly SYNOP data from Neumayer. The $\delta^{18}O$ values represent only periods with snowfall. It has been shown that at Neumayer, the annual mean air temperatures for snowfall conditions are on average approximately 4°C higher than the mean for all days. However, the snowfall temperatures and all-day temperatures show the same temporal variations [*Schlosser*, 1999], which makes the annual means suitable for our comparison.

4.5. SAM Index

As a measure for the influence of the general atmospheric circulation patterns on Fimbul Ice Shelf SMB and $\delta^{18}O$ in accumulated snow, the Southern Annular Mode (SAM) was examined. The SAM is the dominant mode of atmospheric variability in the extratropical Southern Hemisphere. It is revealed as the leading empirical orthogonal function in surface pressure, geopotential height, surface temperature, zonal wind, and many other atmospheric fields [*Thompson and Wallace*, 2000; *Marshall*, 2003]. The state of SAM also influences the large-scale variability of the Southern Ocean [*Hall and Visbeck*, 2002]. Pressure fields from global reanalysis data commonly used to study the SAM are known to have relatively large errors in the polar regions [*Marshall*, 2003]. Therefore, Marshall defined a SAM index based on surface observations, namely, the pressure difference between 40°S and 65°S. He calculated a zonal mean for each of the two latitudes using data from six midlatitude stations (for more details, see *Marshall* [2003]). Basically, a strong meridional pressure gradient corresponds to a positive SAM index and vice versa, the first meaning strong, mostly zonal westerlies and comparatively little exchange of moisture and energy between middle and high latitudes, which leads to a cooling of Antarctica, except for the Antarctic Peninsula that projects into the westerlies.

To investigate the relationship between SAM and SMB/$\delta^{18}O$ from the cores, in this study we used the annual mean SAM index defined by *Marshall* [2003] and provided by the British Antarctic Survey (BAS) at http://www.antarctica.ac.uk/met/gjma/sam.html.

4.6. Dating of the Cores

For dating of the cores, we used seasonal variations of both $\delta^{18}O$ and conductivity from DEP measurements. Figure 2 shows the stable oxygen isotope profiles ($\delta^{18}O$) of the firn cores from eastern Fimbul Ice Shelf, G7, G8, S32, and LP1. The seasonal variations of the stable isotope ratios were in most cases clear enough for annual layer counting. Ambiguities remain mainly in the uppermost parts of the cores due to poorer core quality. This refers to the most recent 3–4 years.

Figure 3a shows the results of the DEP measurements for the Group 2 cores G7, G8, and LP1, as well as S32. Generally, the data are fairly noisy, similar to the western core data (G3, G4, G5, and M2) [see *Schlosser et al.*, 2012]. Thus, an independent dating based on conductivity only would be very difficult. However, by combining of DEP, stable oxygen, and ground-penetrating radar (GPR) data, it was possible to identify peaks that are most likely caused by volcanic fallout. During the time period covered by the cores (1981–2009),

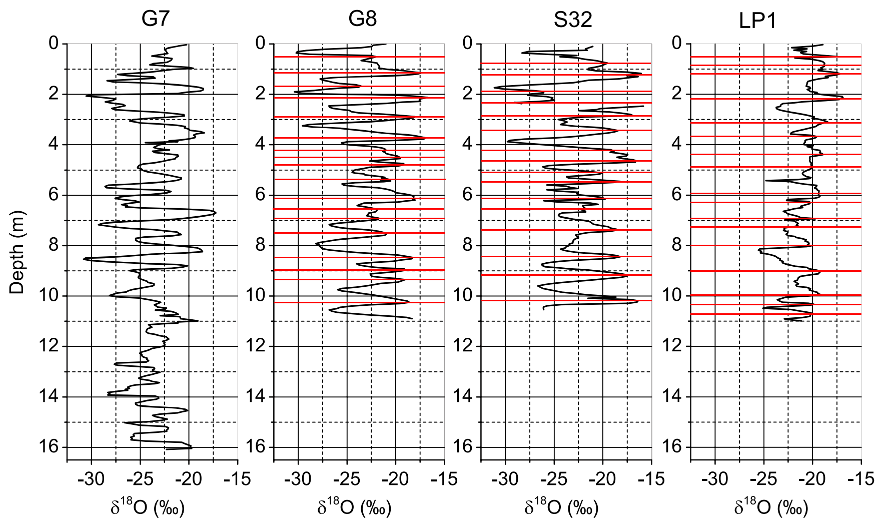

Figure 2. δ^{18}O depth profiles of the Group 2 firn cores G7, G8, S32, and LP1. Stable isotope ratios vary between about −30‰ and −15‰. Seasonal variations are clearly visible and used for dating. Sampling interval was 5 cm, corresponding to approximately 10−12 samples/yr.

two large volcanic eruptions occurred, that of Pinatubo, Philippines (1991), and El Chichon, Mexico (1982). The time of deposition of volcanic material is usually assumed to be 1–2 years after the eruption. However, it depends on the distance between the volcano and the core sites and the transport mechanism in the time following the eruption. We here associate the Pinatubo signal with 1992, the El Chichon signal with 1983.

Figure 3b illustrates the cross-checking of the DEP dating using the GPR measurements for the M2, G5, and G7 cores: the results of the DEP measurements for those cores are shown. These cores are shown because, of the so far unpublished cores, only G7 could be directly connected to the cores M2 and G5 of Group 1. The pronounced peaks marked by red ellipses that can be seen in the conductivity records of all three cores were interpreted as caused by the eruption of El Chichon. The horizon associated to this peak could be followed in the GPR data between these cores [*Sinisalo et al.*, 2013] and agreed well with the corresponding δ^{18}O dating in M2 and G5. Its depth varies from core to core according to the different mean accumulation rates. In G7, the conductivity peak found at about 11 m depth at first sight would be attributed to Pinatubo. However, the radar layer tracking between M2, G5, and G7 strongly suggests it to be El Chichon [*Sinisalo et al.*, 2013]. Comparison to the δ^{18}O annual layer counting reveals that five to nine annual layers likely are missing almost completely. G7 is located close to the grounding line (see Figure 1) and therefore strongly influenced by katabatic winds. Thus, negative SMB values can occur here, which is also confirmed by the stake data from this area [*Sinisalo et al.*, 2013]. For this reason, we cannot calculate annual values of SMB and δ^{18}O for G7 and can only provide the mean annual SMB between 1983 and 2009 using the El Chichon time marker.

Compared to the original dating of the western cores in *Schlosser et al.* [2012], a slight adjustment (within the error bounds) was done in the dating of G4, G5, and M2. This added one additional year to G4 and two to G5 and M2, which improved the agreement with the dating using DEP measurements. Different from the earlier dating, now also the results of the radar measurements could be included, which increased the confidence in the El Chichon peak in spite of the generally noisy character of the DEP data. By layer tracking, this peak could be confirmed at the depth corresponding to the δ^{18}O dating for several cores. The error in the δ^{18}O dating is estimated as 2 years for single years and approximately 3–4 years for the age of the core. This estimate stems from the number of annual layers whose δ^{18}O variations could not be unambiguously identified as seasonal variations and the fact that some of the errors for single years offset each other. Thus, the total error for the core is not the product of “number of years” and “error for single years”; e.g., if two annual layers were mistakenly counted as one year, all subsequent annual layers would have an error of −1 year; if then one annual layer with a major and minor δ^{18}O peak were counted as two years, the total error for the core would be zero. In addition, the error increases with length/age of the core.

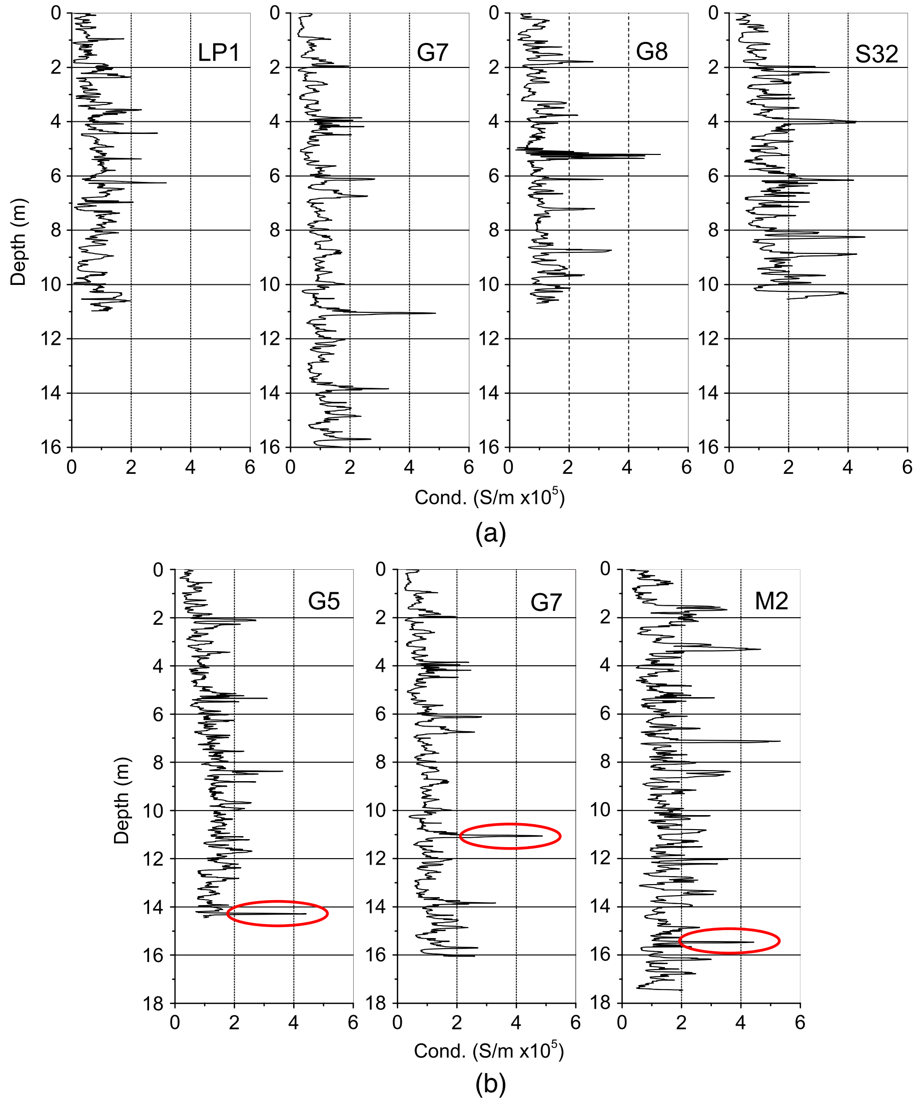

Figure 3. (a) Depth profile of electrical conductivity from DEP of the Group 2 cores LP1, G7, G8, S32. (b) Depth profile of electrical conductivity from DEP of G5, G7, and M2. Red circles mark the peak attributed to the eruption of El Chichon. The corresponding layer in the radar profiles could be tracked between those cores.

4.7. Determination of SMB

The mean annual surface mass balance (SMB) was calculated using the dating described above and the bulk density, which had been determined directly in the field from weighing/measuring core pieces (10 to 50 cm length). The bulk density was smoothed by a polynomial function to take into account the melt layers. For the uppermost layer (~40 cm), density measurements from snow pits dug at the corresponding drilling site were used.

The SMB of the ice shelf is the sum of accumulation and ablation, where accumulation is the sum of precipitation, deposition of hoarfrost, and deposition of snow due to snowdrift, whereas ablation is the sum of sublimation and erosion due to snowdrift. All melted snow refreezes locally, so no runoff is observed. In all cores, numerous ice layers were found, ranging in thickness from 1 mm to several centimeters, the thickest ones reached more than 10 cm. It is assumed that this melting occurred during summer within one annual layer or at the summer boundary of two consecutive layers, so no mass transport from one annual layer to deeper layers occurred. Model results have suggested sublimation values representing to up to approximately 40% of precipitation [*Bromwich et al.*, 2004]. This value represents the upper limit and is usually connected to the occurrence of strong katabatic winds. For the most parts of Fimbulisen, a good

10.1002/2013JD020818

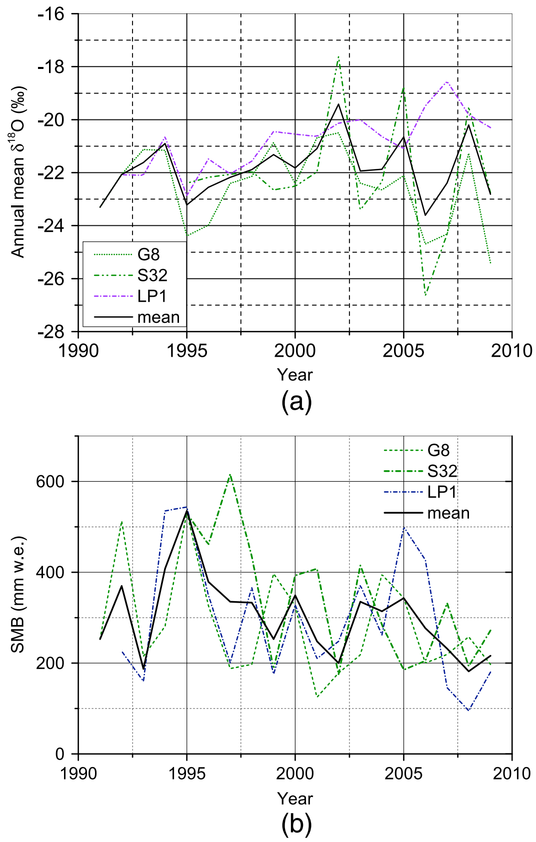

Figure 4. (a) Time series of mean annual $\delta^{18}O$ of the Group 2 cores G8, S32, and LP1 and stacked (mean) record of these cores. (b) Time series of annual SMB of the Group 2 cores G8, S32, and LP1 and stacked (mean) record of these cores.

estimate would be 10–20% [e.g., *Van de Berg et al.*, 2005]; however, higher values can occur at the southern edge of the ice shelf.

A fairly unknown process is the local cycle of sublimation and deposition, which is more important on the dry plateau than on small ice shelves, but does have an influence over Fimbul Ice Shelf mainly during clear weather periods in winter. For those reasons, the SMB cannot directly be taken as a measure for precipitation, even though it is closely related.

5. Results

5.1. SMB and Stable Isotope Ratios

Figure 4 shows the time series of annual mean $\delta^{18}O$ (Figure 4a) and of annual mean SMB (Figure 4b) for the Group 2 firn cores G8, S32, and LP1, including the corresponding stacked records of these cores. Since all cores have similar mean SMBs and are situated in the same climate regime, the stacked record was calculated as arithmetic mean of the values of the single cores (rather than calculating deviations from the corresponding mean values). The stable isotope ratios exhibit a similar temporal variability in all cores, except for the most recent part of the core LP1, where its annual mean $\delta^{18}O$ deviates substantially from the corresponding values of G8 and S32. This most likely has to be attributed to poorer core quality of the layers close to the surface. All curves exhibit relatively high interannual variations in stable oxygen isotope ratio; no statistically significant trend can be found.

Both the temporal and spatial variability of the SMB (Figure 4b) are fairly high: the interannual variability in the stack of SMB series is larger than 30% of the mean value. In order to quantify the spatial variability in the annual SMB, we used the variance separation approach of *Fisher et al.* [1985]. The estimated average signal-to-noise ratio of 0.32 suggests that 70% of the SMB variability in the individual core series can be ascribed to local factors affecting the resulting annual SMB. The main factor influencing the SMB is precipitation, which, in coastal Antarctica, is related to cyclones moving from west to east, north of the coast. These cyclones and thus accumulation are irregular and highly variable [*King and Turner*, 1997; *Schlosser et al.*, 2008; *Simmonds et al.*, 2003]. Additionally, precipitation events are usually accompanied by strong winds, which also increases the spatial variability of SMB due to blowing and drifting snow. Katabatic winds during dry periods can lead to both erosion of the snow surface and deposition of additional snow that is not related to precipitation but is a part of the accumulation. Although katabatic winds do not develop on ice shelves, they can still have an influence on ice shelves with small north-south extent, especially at the southern boundaries, in this case particularly at the location of G7. Further mass loss is due to sublimation of blowing or falling snow. Thus, usually even accumulation rates of closely neighbored cores do not agree well [e.g., *Fisher et al.*, 1985; *Karlöf et al.*, 2005]. *Schlosser and Oerter* [2002a, 2002b] showed that, in spite of the high wind influence, $\delta^{18}O$ values of cores drilled within a short distance usually agree much better than accumulation. The reason for this is most likely that the isotope ratios are relatively uniform during single-precipitation events, whereas accumulation is dependent on wind and topography and can be altered even by extremely slight depressions or rises of the surface [e.g., *Frezzotti et al.*, 2007]. The history of

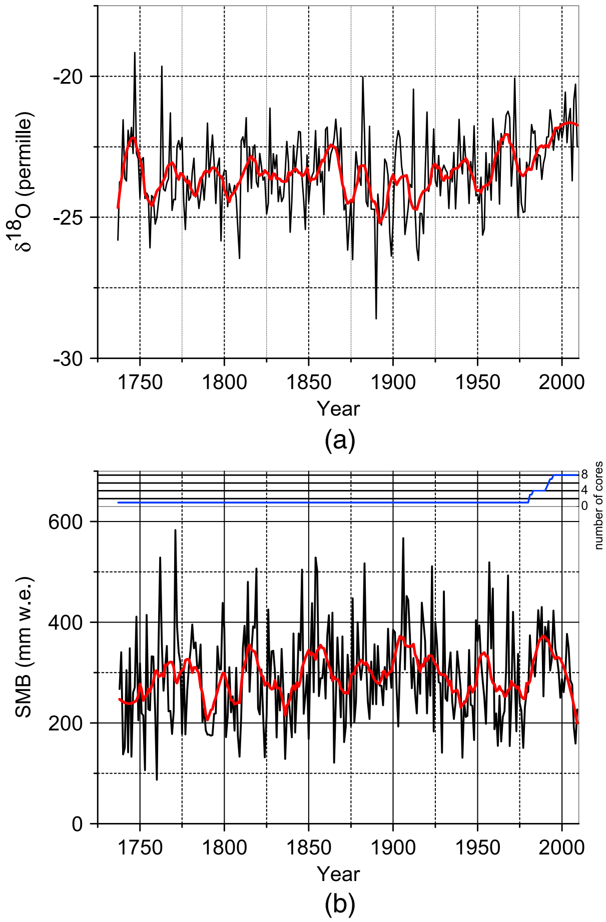

Figure 5. (a) Combined time series 1737–2009 of annual mean δ^{18}O for all Fimbul cores. (b) Combined time series 1737–2009 of annual mean SMB for all Fimbul cores.

the snow surface also plays a role: if the surface is hard packed by wind or is melting already, there is no mixing between the old and the freshly fallen snow, which also increases the agreement in δ^{18}O of cores from the same area. However, in the present study, the magnitude of the signal-to-noise ratio of 0.3 for δ^{18}O is similar to that of the SMB, which is qualitatively similar to the results of *Fisher et al.* [1985]. In spite of the high temporal variability of SMB, a negative trend is found in the Group 2 cores, which is statistically significant in core S32.

In Table 1, the mean annual SMB values and corresponding linear trends of all Fimbul cores are compared. Since several of the cores are rather short, the mean values and trends are calculated both for the full length of each core and for the common time period 1995–2009 covered by all cores . Note that in this particular case, changing the period by a few years does not change the sign of the trend; it can nevertheless affect the inference on its statistical significance. All individual cores show a weak negative trend in SMB, which for cores G4, M2, and S32 was detected statistically significant with the 95% confidence according to *F* test (for G4 and M2 only when calculated for the full core length).

At the location of LP1, a core of 100 m length had been taken in 1999, labeled S100. By combining the data from S100 with the more recent data, the time series could be extended to the period 1737–2009, providing a longer-term, multidecadal-to-centennial-scale outlook to the data from the core network presented here. Figure 5 illustrates the time series of δ^{18}O (Figure 5a) and SMB (Figure 5b) derived from core S100 and the stacked record of the seven new cores. (The number of cores that were used for calculation of the stacked record varies with time and is shown in the upper part of Figure 5b). Before approximately 1980, the record stems from S100 alone, afterward the number of cores increases according to the age of the shorter cores. From 1993 on, the record contains the data from all cores except G7. The agreement between LP1 and S100 in the overlapping part is not satisfactory. It cannot be quantified, though, how much of the disagreement is due to poor core quality, possible dating errors and real local differences (especially for SMB, the differences between closely neighbored cores can be large). Thus, these data were not omitted. However, these few years of a single core, for which the data are less reliable, do not affect our general results. The dating of the upper part of S100 had been cross-checked using another shallow core drilled in 1997 (S20) [*Isaksson et al.*, 1999]. The mean annual accumulation rates of all three cores (S20, S100, and LP1) agree well within the error bounds (271 (29), 296 (33), and 290 (10), respectively). We use the stacked record rather than only LP1 for the most recent period to create the extended time series. The stacked record was calculated as for Figure 4. Trend analysis for S100 done by *Kaczmarska et al.* [2004] and *Divine et al.* [2009] suggests that statistically significant decline in annual SMB has commenced as early as the 1930s, in parallel with a significantly positive trend in δ^{18}O. Note that when the longer S100 series is omitted from the stack, the statistically significant negative SMB trend remains, while δ^{18}O still shows a weak insignificant yet positive trend.

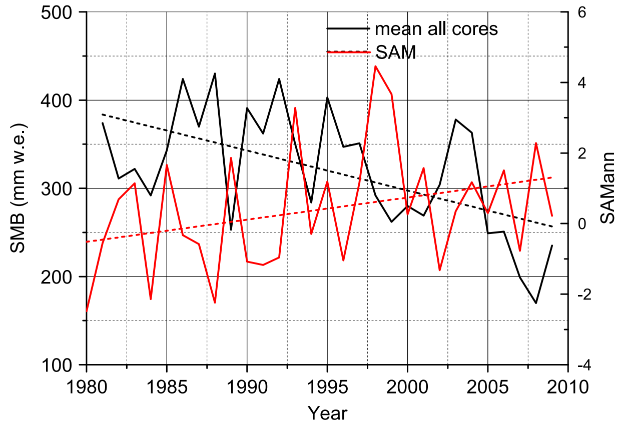

Figure 6. Time series of mean annual SMB (stacked record of all cores) and annual SAM index [*Marshall*, 2003]. The dashed lines show the linear trends for the time series. The positive trend in SAM is not statistically significant over the considered time interval; the negative trend in SMB is statistically significant. SAM and SMB are negatively correlated ($r = -0.382$, $p = 0.04$).

5.2. Relationships Between $\delta^{18}O$, Air Temperature, SMB and the Southern Annular Mode

To relate the observed temporal variations of SMB and $\delta^{18}O$ to the Southern Hemisphere climate variability, the SAM index was chosen as measure for the climate mode. The SAM is the dominant mode but explains only approximately one third of the atmospheric variability in the Southern Hemisphere. Thus, we can only present a quite general discussion here. To take into account all possible influences would be beyond the scope of this study.

Figure 6 demonstrates the stacked record of mean annual SMB from all seven cores compared to the annual SAM index of *Marshall* [2003]. The dashed line represents a linear regression of the time series. Whereas the SAM shows a positive trend (not significant over the time period considered here) that already started around 1965 [e.g., *Marshall*, 2003, 2007], the SMB (averaged over all cores) exhibits a weak but statistically significant negative trend of about 5 mm w.e. yr^{-1} in the past three decades. We note that the trend in SAM for the period analysed in this study can be considered a continuation of the statistically significant change toward more positive SAM mentioned above.

The mean annual stable isotope ratio is commonly assumed to be linearly (positively) related to the annual mean air temperature at the deposition site [*Dansgaard*, 1964]. For an increasing SAM index, a decrease in temperature would be expected in East Antarctica [*Marshall*, 2003, 2007]. Thus, the stacked mean $\delta^{18}O$ record of all cores was compared to the annual mean air temperature at Neumayer station and, again, the annual SAM index in Figure 7. Note that back in 1993, it is the average annual mean of all seven cores; before that, the number of cores decreases corresponding to the age of the cores (see Figure 5b). Figure 7 demonstrates that whereas the air temperature at Neumayer has been stable with only slight variations around the long-term mean of −16.0°C, the $\delta^{18}O$ of the cores shows a weak (statistically not significant) positive trend.

The relationship between mean annual stable oxygen ratios of snow/ice and the annual mean air temperature at the deposition site is used in paleoclimatology to derive past air temperatures from ice cores [*Dansgaard*, 1964]. In ice core science, it is generally also assumed that stable oxygen isotope ratios and accumulation rates are positively correlated. This is due to the dependence of saturation vapor pressure on air temperature and the linear relationship between $\delta^{18}O$ and temperature. However, the latter relationship explains only the thermodynamic part of the behavior of SMB versus temperature or $\delta^{18}O$ and does not take into account any influences of atmospheric dynamics. Seasonality alone could be a reason for the disappearance of the linear relationship between stable isotope ratios and temperature [*Schlosser*, 1999; *Noone et al.*, 1999], and it can also

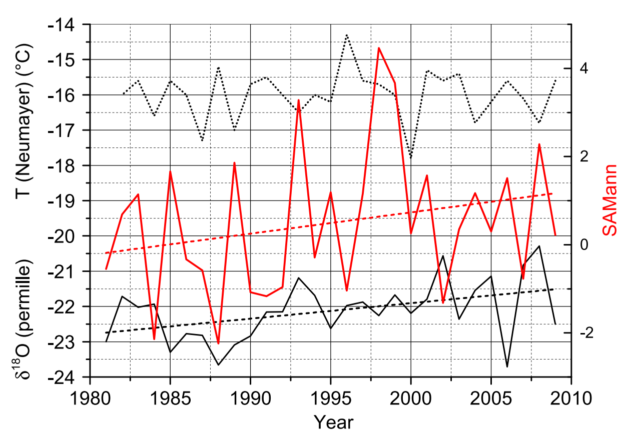

Figure 7. Time series of mean annual $\delta^{18}O$ (stacked record of all cores), annual mean air temperature of Neumayer Station, and annual SAM index. The dashed lines show linear trends for the time series.

strongly influence the correlation between SMB and temperature. Whereas over the considered time period of 1981–2009 the Neumayer air temperature exhibits no significant change and the $\delta^{18}O$ generally shows only a weak, statistically not significant positive trend, the mean SMB derived from the cores exhibits a negative trend, which is statistically significant in three of the seven cores (G4, M2, and S32) and in the stacked record of all cores. The correlation coefficients between SAM, Neumayer temperature, SMB, and $\delta^{18}O$ (stacked record) of the firn cores were calculated. The analysis revealed that none of the correlations between $\delta^{18}O$, SMB, and temperature was statistically significant at the 95% confidence level. Only SAM and SMB show a negative correlation statistically significant at the 95% confidence level ($r = -0.4$, $p = 0.04$). We note, however, that when the linear trends are subtracted from these series, the magnitude of the correlation decreases to a lower yet significant value of -0.3 (at the 90% confidence level).

6. Discussion and Conclusion

All seven investigated firn cores from Fimbul Ice Shelf that could be dated consistently show a weak negative trend in SMB (statistically significant in three cores) and a not statistically significant weak positive trend in $\delta^{18}O$. However, when viewed in a longer-term context, the negative SMB trend and positive $\delta^{18}O$ trend seems to be a continuation of respective statistically significant changes detected between 1930 and 2000 in the S100 core alone by *Kaczmarska et al.* [2004] and *Divine et al.* [2009]. Several other cores in Western DML exhibit similar negative trends in the twentieth century [*Schlosser and Oerter*, 2002a] and in the second half of the twentieth century [*Isaksson et al.*, 1996; *Isaksson and Melvold*, 2002]. A decreasing SMB at the same time as constant or increasing temperature/$\delta^{18}O$ has also been found in several other studies [e.g., *Noone and Simmonds*, 1998; *Divine et al.*, 2009] using model data and firn core data from Dronning Maud Land.

Neumayer mean annual air temperature data for the corresponding time period 1981–2009 covered fully or partly by the Fimbul cores (see Table 1) shows no tendency toward warming or cooling. We refrain from converting the $\delta^{18}O$ record into a temperature record since obviously other factors than temperature are at play. At the same time, the annual SAM index also exhibits a positive trend, although its statistical significance cannot be confirmed for the period of overlap with the stacked series from the presented core network. However, the trend in annual SAM index is statistically significant for the period beginning around 1960. It is beyond the scope of this paper to give a detailed discussion of the Southern Hemisphere climate modes relevant for Antarctic precipitation and thus surface mass balance. However, we would like to put our results into a broader climatic context by discussing possible influences of SAM on firn core properties. Generally, a stronger positive SAM is associated with lower temperatures in Antarctica (with exception of the Antarctic Peninsula) and stronger westerlies in the circumpolar trough [e.g., *Marshall*, 2007; *Russell and McGregor*, 2010]. This so-called high-index circulation means a strong zonal flow with lower-amplitude long waves, thus relatively little exchange of heat and moisture between high and middle latitudes. On the contrary, a negative SAM index is associated with a low-index (meridional) circulation, with the Rossby waves reaching very large amplitudes [*Palmer*, 1998], which leads to large meridional moisture and energy transports. Therefore, a decrease in SMB associated with an increase in the SAM index is plausible, but, in our case, not because temperature, and thus, saturation vapor pressure is decreasing, as usually assumed. Instead, the decreasing meridional moisture flux associated with the increasing SAM index could lead to less precipitation/accumulation in the study area. *Tietäväinen and Vihma* [2008] found that the meridional moisture transport at 60°S has a negative correlation with the SAM index, whereas the zonal moisture transport is positively correlated with the SAM index (both statistically significant at the 95% confidence level). Since the stable isotope ratio at the same time is constant or slightly increasing, it must be concluded that mainly the accumulation/precipitation in the colder seasons is reduced, since this increases the mean annual $\delta^{18}O$ due to a smaller contribution of the coldest periods to the annual mean. However, the positive trend in the annual SAM index is mainly caused by spring and summer conditions.

Apart from changing the seasonality of precipitation, an increase in SAM index (intensified zonal circulation) also causes an increase in contribution of "local" (Southern Ocean) moisture sources to coastal Antarctic precipitation [*Noone and Simmonds*, 2002]. This moisture has a shorter distillation path and is hence less depleted in heavy isotopes than moisture of a midlatitude origin, which means seemingly warmer conditions to be found in the ice cores. This effect would be more important in summer/fall than in winter/spring because of less sea ice coverage, which means more entrainment of additional moisture on the way to the deposition site

[*Noone and Simmonds*, 2004]. For the interior areas, the moisture transport mechanisms are not satisfactorily understood yet. The effects of changed seasonality and changed moisture source are likely to counteract. Therefore, we do not see a statistically robust change in the stable isotope ratio for the period since 1981. In the longer δ^{18}O series of S100, the parallel increase in SAM index and stable isotope ratio is apparent.

We conclude that the observed features in SMB and δ^{18}O thus cannot be explained simply by annual or seasonal SAM indices. A study of SAM at higher temporal resolution and a thorough investigation of other influences like the longer-term changes in SAO (semiannual oscillation) and sea ice extent complemented by General (Atmospheric) Circulation Model modeling with Lagrangian moisture source diagnostic would be necessary to understand the complex relationships.

Our results are contradictory to the assumption of a generally positive correlation between SMB and δ^{18}O, which is commonly used in ice core studies, particularly in flow models for dating of the cores. Of course, Figures 6 and 7 cover only approximately three decades and Fimbul Ice Shelf is representative for the small Eastern Antarctic ice shelves, but not for the East Antarctic ice sheet, where the deep ice cores are drilled. However, the physical processes that influence SMB and δ^{18}O are basically the same for the different time periods and areas. Interannual differences in today's atmospheric circulation can cause differences in the annual SMB and stable isotope ratios in a way qualitatively analogous to the effect of glacial/interglacial changes in general atmospheric circulation on ice core properties; e.g., in a glacial period, a northward shift of the westerlies might have happened. Today, in an extreme year we might find conditions with westerlies far more north than usually and we can study qualitatively the effects of this circulation change on moisture transport, precipitation regime, and thus stable isotopes. In fact, the extreme modern year will most likely show just the lower limit of a possible northward shift in a glacial period. But such a study would enable us to assess the direction of the change in the processes related to precipitation and consequently stable water isotopes. For the relationship between temperature and SMB, additionally to the thermodynamics, the dynamic influences have to be considered. Without information about paleoatmospheric dynamics, we need to conclude from studies of modern processes to the past conditions.

On a larger scale, recent studies of Antarctic precipitation do not confirm a general negative trend. *Monaghan et al.* [2006] found no significant trend in Antarctic snowfall in the past 50 years, which is matched by a constant temperature in East Antarctica in the past 50 years [*Turner et al.*, 2002, 2005]. *Nicolas and Bromwich* [2011] warned to be cautious with trend analysis using reanalysis data. In the most reliable reanalysis, the ERA-interim, they did not find any significant trend in precipitation minus evaporation for the last 20 years. However, *Monaghan et al.* [2008] detected a hint of warming since 1992; three out of fifteen investigated Antarctic stations (coastal and continental) exhibited a statistically significant warming trend.

Further monitoring of Antarctic temperature and ice dynamics, particularly at the coasts/on the ice shelves, is necessary to obtain a less ambiguous picture and to be able to assess the consequences for sea level change.

Acknowledgments
We are grateful to all members of the Fimbul Ice Shelf Expeditions 2009/2010 and 2010/2011 for various support in the field. Neumayer SYNOP data were kindly provided by Gert König-Langlo, AWI, Bremerhaven. BAS is acknowledged for providing the SAM index data online. We thank three anonymous reviewers for their thorough reviews that helped improving this paper. This study was financed by the Norwegian Research Council through NARE, Center for Ice, Climate and Ecosystems (ICE) at the Norwegian Polar Institute, Tromsø, the EU Regional Development Foundation, project3.2.0801.12-0044, and the Austrian Science Fund (FWF) (grants V31-N10/P24223). The core data are available at Norwegian Polar Institute (Elisabeth.Isaksson@npolar.no).

References

Bintanja, R., G. J. van Oldenborgh, S. S. Drijfhout, B. Wouters, and C. A. Katsman (2013), Important role for ocean warming and increased ice-shelf melt in Antarctic sea ice expansion, *Nat. Geosci.*, *6*, 376–379.

Boening, C., M. Lebsock, F. Landerer, and G. Stephens (2012), Snowfall-driven mass change on the East Antarctic ice sheet, *Geophys. Res. Lett.*, *39*, L21501, doi:10.1029/2012GL053316.

Bromwich, D. H., Z. Guo, L. Bai, and Q.-S. Chen (2004), Modeled Antarctic Precipitation. Part I: Spatial and temporal variability, *J. Clim.*, *17*, 427–447.

Bromwich, D. H., J. P. Nicolas, A. J. Monaghan, M. A. Lazzara, L. M. Keller, G. A. Weidner, and A. B. Wilson (2013), Central West Antarctica among the most rapidly warming regions on Earth, *Nat. Geosci.*, *6*, 139–144, doi:10.1038/NGEO1671.

Dansgaard, W. (1964), Stable isotopes in precipitation, *Tellus*, *16*(4), 436–468.

Depoorter, M. A., J. L. Bamber, J. A. Griggs, J. T. M. Lenaerts, S. R. M. Ligtenberg, M. R. van den Broeke, and G. Moholdt (2013), Calving fluxes and basal melt rates of Antarctic ice shelves, *Nature*, *502*(7469), 89–92, doi:10.1038/nature12567.

Divine, D. V., E. Isaksson, M. Kaczmarska, F. Godtliebsen, H. Oerter, E. Schlosser, S. J. Johnsen, M. van den Broeke, and R. S. W. Van de Wal (2009), Tropical Pacific—High latitude south Atlantic teleconnections as seen in the δ^{18}O variability in Antarctic coastal ice cores, *J. Geophys. Res.*, *114*, D11112, doi:10.1029/2008JD01047.

Fisher, D. A., N. Reeh, and H. B. Clausen (1985), Stratigraphic noise in time series derived from ice cores, *Ann. Glaciol.*, *7*, 76–83.

Frezzotti, M., S. Urbini, M. Proposito, C. Scarchilli, and S. Gandolfi (2007), Spatial and temporal variability of surface mass balance near Talos Dome, East Antarctica, *J. Geophys. Res.*, *112*, F02032, doi:10.1029/2006JF000638.

Glen, J., and J. Paren (1975), The electrical properties of snow and ice, *J. Glaciol.*, *15*(73), 15–38.

Gorodetskaya, I. V., N. P. M. Van Lipzig, M. R. Van den Broeke, A. Mangold, W. Boot, and C. H. Reijmer (2013), Meteorological regimes and accumulation patterns at Utsteinen, Dronning Maud Land, East Antarctica: Analysis of two contrasting years, *J. Geophys. Res. Atmos.*, *118*, 1–16, doi:10.1002/jgrd.50177.

Hall, A., and M. Visbeck (2002), Synchronous variability in the Southern Hemisphere atmosphere, sea ice, and ocean resulting from the Annular Mode, *J. Clim.*, *15*, 3043–3057.
Hattermann, T., O.-A. Nøst, J. M. Lilly, and L. H. Smedsrud (2012), Two years of oceanic observations below Fimbul Ice Shelf, Antarctica, *Geophys. Res. Lett.*, *39*, L12605, doi:10.1029/2012GL051012.
Isaksson, E., and K. Melvold (2002), Trends and patterns in the recent accumulation and oxygen isotopes in coastal DML, Antarctica: Interpretations from shallow firn cores, *Ann. Glaciol.*, *35*, 175–180.
Isaksson, E., W. Karlén, N. Gundestrup, P. Mayewski, S. Whitlow, and M. Twickler (1996), A century of accumulation and temperature changes in Dronning Maud Land, Antarctica, *J. Geophys. Res.*, *101*(D3), 7085–7094, doi:10.1029/95JD03232.
Isaksson, E., M. R. Van den Broeke, J. G. Winther, L. Karlöf, J. F. Pinglot, and N. Gundestrup (1999), Accumulation and proxy-temperature variability in Dronning Maud Land, Antarctica, determined from shallow firn cores, *Ann. Glaciol.*, *29*, 17–22.
Jacobs, S. S., A. Jenkins, C. F. Giulivi, and P. Dutrieux (2011), Stronger ocean circulation and increased melting under Pine Island Glacier ice shelf, *Nat. Geosci.*, *4*, 519–523.
Jenkins, A., P. Dutrieux, S. S. Jacobs, S. D. McPhail, J. R. Perrett, A. T. Webb, and D. White (2010), Observations beneath Pine Island Glacier in West Antarctica and implications for its retreat, *Nat. Geosci.*, *3*(7), 468–472, doi:10.1038/ngeo890.
Kaczmarska, M., et al. (2004), Accumulation variability derived from an ice core from coastal DML, Antarctica, *Ann. Glaciol.*, *39*, 339–345.
Kaczmarska, M., E. Isaksson, L. Karlöf, O. Brandt, J.-G. Winther, R. S. W. Van de Wal, M. Van den Broeke, and S. J. Johnsen (2006), Ice core melt features in relation to Antarctic coastal climate, *Antarct. Sci.*, *18*(2), 271–278.
Karlöf, L., et al. (2005), Accumulation variability over a small area in east DML, Antarctica, as determined from shallow firn cores and snow pits: some implications for ice-core records, *J. Glaciol.*, *51*(174), 343–352.
King, J., and J. Turner (1997), *Antarctic Meteorology and Climatology*, 409 pp., Cambridge Univ. Press, Cambridge.
Langley, K., A. Von Deschwanden, J. Kohler, A. Sinisalo, K. Matsuoka, and O.-A. Nøst (2014), Complex network of channels beneath an Antarctic ice shelf, *Geophys. Res. Lett.*, *41*, 1209–1215, doi:10.1002/2013GL058947.
Lenaerts, J. T. M., E. van Meijgaard, M. R. van den Broeke, S. R. M. Ligtenberg, M. Horwarth, and E. Isaksson (2013), Recent snowfall anomalies in Dronning Maud Land, East Antarctica, in a historical and future climate perspective, *Geophys. Res. Lett.*, *40*, 2684–2688, doi:10.1002/grl.50559.
Lunde, T. (1961), On the snow accumulation in Dronning Maud Land. Den Norske Antarktisekspedisjon 1956-60. Scientific Results I. Nor. Polarinst. Skr., 123, 48 pp.
Marshall, G. (2003), Trends in the Southern Annular Mode from observations and reanalyses, *J. Clim.*, *16*, 4134–4143.
Marshall, G. (2007), Half-century seasonal relationships between the Southern Annular Mode and Antarctic temperatures, *Int. J. Climatol.*, *27*, 373–383, doi:10.1002/joc.1407.
Melvold, K. (1999), Impact of recent climate on glacier mass balance: Studies on Kongsvegen, Svalbard and Jutulstraumen, Antarctica. PhD thesis, Department of Geography Report 13. University of Oslo.
Melvold, K., J.-O. Hagen, J. F. Pinglot, and N. Gundestrup (1998), Large spatial variation in accumulation rate in Jutulstraumen ice stream, Dronning Maud Land, Antarctica, *Ann. Glaciol.*, *27*, 231–238.
Mitchell, J. M., Jr., B. Dzerdzeevskii, H. Flohn, W. L. Hofmeyr, H. H. Lamb, K. N. Rao, and C. C. Walléen (1966), Climatic Change. Report of a working group of the Commission for Climatology. *Tech. Note 79*, WMO No. 195. 79 pp.
Monaghan, A. J., D. H. Bromwich, and S. Wang (2006), Recent trends in Antarctic snow accumulation from Polar MM5 simulations, *Philos. Trans. R. Soc. A*, *364*, 1683–1708.
Monaghan, A. J., D. H. Bromwich, W. Chapman, and J. C. Comiso (2008), Recent variability and trends of Antarctic near-surface temperature, *J. Geophys. Res.*, *113*, D04105, L21501, doi:10.1029/2007JD009094.
Moore, J. C., R. Mulvaney, and J. G. Paren (1989), Dielectric stratigraphy of ice: A new technique for determining total ionic concentrations in polar ice, *Geophys. Res. Lett.*, *16*(10), 1177–1180, doi:10.1029/GL016i010p01177.
Neethling, D. C. (1970), Snow accumulation on the Fimbul Ice Shelf, western Dronning Maud Land, Antarctica, in *International Symposium on Antarctic Glaciological Exploration (ISAGE)*, vol. 86, edited by A. J. Gow et al., pp. 390–404, Int. Assoc. of Hydrol. Sci., Cambridge.
Nicolas, J. P., and D. H. Bromwich (2011), Precipitation changes in high southern latitudes from global reanalyses: A cautionary tale, *Surv. Geophys.*, *32*, 475–494, doi:10.1007/s10712-011-9114-6.
Noone, D., and I. Simmonds (1998), Implications for the interpretation of ice-core isotope data from analysis of modeled Antarctic precipitation, *Ann. Glaciol.*, *27*, 398–402.
Noone, D., and I. Simmonds (2002), Annular variations in moisture transport mechanisms and the abundance of $\delta^{18}O$ in Antarctic snow, *J. Geophys. Res.*, *107*(D24), 4742, doi:10.1029/2002JD002262.
Noone, D., and I. Simmonds (2004), Sea ice control of water isotope transport to Antarctica and implications for ice core interpretation, *J. Geophys. Res.*, *109*, D07105, doi:10.1029/2003JD004228.
Noone, D., J. Turner, and R. Mulvaney (1999), Atmospheric signals and characteristics of accumulation in Dronning Maud Land, Antarctica, *J. Geophys. Res.*, *104*(D16), 19,191–19,211, doi:10.1029/1999JD900376.
Palmer, T. N. (1998), Nonlinear dynamics and climate change: Rossby's legacy, *Bull. Am. Meteorol. Soc.*, *79*(7), 1411–1423.
Park, J. W., N. Gourmelen, A. Shepherd, S. W. Kim, D. G. Vaughan, and D. J. Wingham (2013), Sustained retreat of the Pine Island Glacier, *Geophys. Res. Lett.*, *40*, 1–6, doi:10.1002/grl.50379.
Pritchard, H. D., R. J. Arthern, D. G. Vaughan, and L. A. Edwards (2009), Extensive dynamic thinning on the margins of the Greenland and Antarctic ice sheets, *Nature*, *461*, 971–975.
Pritchard, H. D., S. R. M. Ligtenberg, H. A. Fricker, D. G. Vaughan, M. R. Van den Broeke, and L. Padman (2012), Antarctic ice sheet loss driven by basal melting of ice shelves, *Nature*, *484*, 502–505.
Rignot, E. (2008), Changes in West Antarctic ice stream dynamics observed with ALOS PALSAR data, *Geophys. Res. Lett.*, *35*, L12505, doi:10.1029/2008GL033365.
Rignot, E., S. Jacobs, J. Mouginot, and B. Scheuchl (2013), Ice-shelf melting around Antarctica, *Science*, *341*, 266–270, doi:10.1126/science.1235798.
Rolstad, C., I. Whillans, J. O. Hagen, and E. Isaksson (2000), Large-scale force budget of an outlet-glacier: Jutulstraumen, Dronning Maud Land, *Ann. Glaciol.*, *30*, 123–128.
Rotschky, G., P. Holmlund, E. Isaksson, R. Mulvaney, M. Van den Broeke, and J.-G. Winther (2007), A new surface accumulation map for western Dronning Maud Land, Antarctica, from interpolation of point measurements, *J. Glaciol.*, *53*(182), 385–398.
Rott, H., W. Rack, P. Skvarca, and H. De Angelis (2002), Northern Larsen Ice Shelf, Antarctica: Further retreat after collapse, *Ann. Glaciol.*, *34*, 277–282.
Rott, H., T. Nagler, and W. Rack (2007), Increased export of grounded ice after the collapse of northern Larsen ice shelf, Antarctic Peninsula, observed by Envisat ASAR, *Proc IGARSS*, 1174–1176, doi:10.1109/IGARSS.2007.4423013.

Russell, A., and G. R. McGregor (2010), Southern hemisphere atmospheric circulation: Impacts on Antarctic climate and reconstructions from Antarctic ice core data, *Clim. Change*, *99*, 155–192, doi:10.1007/s10584-009-9673-4.

Schlosser, E. (1999), Effects of seasonal variability of accumulation on yearly mean $\delta^{18}O$ values in Antarctic snow, *J. Glaciol.*, *45*(151), 463–468.

Schlosser, E., and H. Oerter (2002a), Seasonal variations of accumulation and the isotope record in ice cores: A study with surface snow samples and firn cores from Neumayer Station, Antarctica, *Ann. Glaciol.*, *35*, 97–101.

Schlosser, E., and H. Oerter (2002b), Shallow firn cores from Neumayer, Ekströmisen, Antarctica: A comparison of accumulation rates and stable-isotope ratios, *Ann. Glaciol.*, *35*, 91–96.

Schlosser, E., M. G. Duda, J. G. Powers, and K. W. Manning (2008), The precipitation regime of Dronning Maud Land, Antarctica, derived from AMPS (Antarctic Mesoscale Prediction System) Archive Data, *J. Geophys. Res.*, *113*, D24108, doi:10.1029/2008JD009968.

Schlosser, E., H. Anschütz, E. Isaksson, T. Martma, D. Divine, and O.-A. Nøst (2012), Surface mass balance and stable oxygen isotope ratios from shallow firn cores on Fimbulisen, East Antarctica, *Ann. Glaciol.*, *53*(60), 70–78, doi:10.3189/2012AoG60A102.

Simmonds, I., K. Keay, and E. Lim (2003), Synoptic activity in the seas around Antarctica, *Mon. Weather Rev.*, *131*, 272–288.

Sinisalo, A., et al. (2013), Surface mass balance on Fimbul ice shelf, East Antarctica: Comparison of field measurements and large scale studies, *J. Geophys. Res. Atmos.*, *118*, 1–11, doi:10.1002/jgrd.50875.

Solomon, S., D. Qin, M. Manning, Z. Chen, M. Marquis, K. B. Averyt, M. Tignor, and H. L. Miller (2007), *Climate Change 2007: The Physical Science Basis, Contribution of Working Group I to the Fourth Assessment Report of the Intergovernmental Panel on Climate Change*, Cambridge Univ. Press, Cambridge, U. K., and New York.

Swithinbank, C. W. M. (1957), The regime of the ice shelf at Maudheim as shown by stake measurements. Norwegian-British-Swedish Antarctic Expedition 1949-1952, in *Scientific Results*, Glaciol. INorsk Polarinstitutt, Oslo, vol. 3, pp. 41–75.

Thompson, D. W. J., and J. M. Wallace (2000), Annular modes in the extratropical circulation. Part 1: Month-to month variability, *J. Clim.*, *13*, 1000–1016.

Tietäväinen, H., and T. Vihma (2008), Atmospheric moisture budget over Antarctica and the Southern Ocean on the basis of ERA-40 reanalysis, *Int. J. Climatol.*, *28*, 1977–1995.

Turner, J., S. R. Colwell, J. C. King, T. A. Lachlan-Cope, and P. D. Jones (2002), Recent temperature trends in the Antarctic, *Nature*, *418*, 291–292.

Turner, J., S. R. Colwell, G. J. Marshall, T. A. Lachlan-Cope, A. M. Carleton, P. D. Jones, V. Lagun, P. A. Reid, and S. Iagovkina (2005), Antarctic climate change during the last 50 years, *Int. J. Climatol.*, *25*, 279–294.

Van de Berg, W. J., M. R. Van Den Broeke, C. H. Reijmer, and E. Van Meijgaard (2005), Characteristics of the Antarctic surface mass balance, 1958–2002, using a regional atmospheric model, *Ann. Glaciol.*, *41*, 97–104.

Van Loon, H. (1967), The half-yearly oscillations in middle and high southern latitudes and the coreless winter, *J. Atmos. Sci.*, *24*, 472–86.

Wilhelms, F. (2005), Explaining the dielectric properties of firn as a density-and-conductivity mixed permittivity (DECOMP), *Geophys. Res. Lett.*, *32*, L16501, doi:10.1029/2005GL022808.

Wilhelms, F., J. Kipfstuhl, H. Miller, H. Heinloth, and J. Firestone (1998), Precise dielectric profiling of ice cores: A new device with improved guarding and its theory, *J. Glaciol.*, *44*(146), 171–174.

